remote sensing

MDPI

Article

Forest Restoration Monitoring Protocol with a Low-Cost Remotely Piloted Aircraft: Lessons Learned from a Case Study in the Brazilian Atlantic Forest

Rafael Walter Albuquerque [1,*], Manuel Eduardo Ferreira [2], Søren Ingvor Olsen [3], Julio Ricardo Caetano Tymus [4], Cintia Palheta Balieiro [4], Hendrik Mansur [4], Ciro José Ribeiro Moura [5,6], João Vitor Silva Costa [2], Maurício Ruiz Castello Branco [7] and Carlos Henrique Grohmann [1]

1 Institute of Energy and Environment, University of São Paulo, Prof. Luciano Gualberto Avenue, 1289, Butanta 05508-010, SP, Brazil; guano@usp.br
2 Instituto de Estudos Socioambientais—IESA, Laboratório de Processamento de Imagens e Geoprocessamento—LAPIG/Pro-Vant, Universidade Federal de Goiás—UFG, Campus II, Cx. Postal 131, Goiás 74001-970, GO, Brazil; manuel@ufg.br (M.E.F.); joao_vitor@discente.ufg.br (J.V.S.C.)
3 Department of Computer Science (DIKU), University of Copenhagen, Universitetsparken 1, 2100 Ø Copenhagen, Denmark; ingvor@di.ku.dk
4 The Nature Conservancy Brasil—TNC, Av. Paulista, 2439/91, Bela Vista 01311-300, SP, Brazil; jtymus@tnc.org (J.R.C.T.); cbalieiro@tnc.org (C.P.B.); hmansur@tnc.org (H.M.)
5 Programa de Engenharia Ambiental, Av. Athos da Silveira Ramos, 149, Ilha do Fundão, Centro de Tecnologia—Bloco A, 2º andar, Sala DAPG—Universidade Federal do Rio de Janeiro, Escola Politécnica 21941-909, RJ, Brazil; ciro@poli.ufrj.br
6 Instituto Estadual do Ambiente—INEA, Av. Venezuela, 110, Saúde 20081-312, RJ, Brazil
7 Instituto Terra de Preservação Ambiental—ITPA, Rua Francisco Alves, 53, Miguel Pereira 26900-000, RJ, Brazil; mauricio@itpa.org.br
* Correspondence: rafael.albuquerque@usp.br

Abstract: Traditional forest restoration (FR) monitoring methods employ spreadsheets and photos taken at the ground level. Since remotely piloted aircraft (RPA) generate a panoramic high resolution and georeferenced view of the entire area of interest, this technology has high potential to improve the traditional FR monitoring methods. This study evaluates how low-cost RPA data may contribute to FR monitoring of the Brazilian Atlantic Forest by the automatic remote measurement of Tree Density, Tree Height, Vegetation Cover (area covered by trees), and Grass Infestation. The point cloud data was processed to map the Tree Density, Tree Height, and Vegetation Cover parameters. The orthomosaic was used for a Random Forest classification that considered trees and grasses as a single land cover class. The Grass Infestation parameter was mapped by the difference between this land cover class (which considered trees and grasses) and the Vegetation Cover results (obtained by the point cloud data processing). Tree Density, Vegetation Cover, and Grass Infestation parameters presented F_scores of 0.92, 0.85, and 0.64, respectively. Tree Height accuracy was indicated by the Error Percentage considering the traditional fieldwork and the RPA results. The Error Percentage was equal to 0.13 and was considered accurate because it estimated a 13% shorter height for trees that averaged 1.93 m tall. Thus, this study showed that the FR structural parameters were accurately measured by the low-cost RPA, a technology that contributes to FR monitoring. Despite accurately measuring the structural parameters, this study reinforced the challenge of measuring the Biodiversity parameter via remote sensing because the classification of tree species was not possible. After all, the Brazilian Atlantic Forest is a biodiversity hotspot, and thus different species have similar spectral responses in the visible spectrum and similar geometric forms. Therefore, until improved automatic classification methods become available for tree species, traditional fieldwork remains necessary for a complete FR monitoring diagnostic.

Keywords: Atlantic Forest; drones; SfM-MVS; structural parameters; unmanned aerial vehicle

Citation: Albuquerque, R.W.; Ferreira, M.E.; Olsen, S.I.; Tymus, J.R.C.; Balieiro, C.P.; Mansur, H.; Moura, C.J.R.; Costa, J.V.S.; Branco, M.R.C.; Grohmann, C.H. Forest Restoration Monitoring Protocol with a Low-Cost Remotely Piloted Aircraft: Lessons Learned from a Case Study in the Brazilian Atlantic Forest. *Remote Sens.* **2021**, *13*, 2401. https://doi.org/10.3390/rs13122401

Academic Editor: Giovanni Santopuoli and Kim Calders

Received: 27 April 2021
Accepted: 15 June 2021
Published: 19 June 2021

1. Introduction

Remotely piloted aircraft (RPA), popularly known as drones, present notable technical advantages in several fields, such as journalism [1] and agriculture [2]. Nevertheless, in Forest Restoration (FR) projects, the real benefits that RPA can provide still demand more studies.

Traditional FR monitoring methods employ sheets and photos taken at the ground level that do not register the whole area of an FR project, e.g., the methods described in the FR monitoring protocol of the Brazilian Atlantic Forest biome [3]. According to Viani et al. [4], the Atlantic Forest FR monitoring protocol is excellent because it provides data collection standards to avoid biases and subjectivity. As the scope of future studies, the authors stated that an automatic feedback report would improve the FR monitoring protocol. Therefore, it would be interesting to investigate whether RPA is capable of generating an automatic feedback report to efficiently support FR monitoring.

Since RPA generates a panoramic high resolution and georeferenced view of the entire area of interest [5], this technology has high potential to promote efficient FR monitoring [6]. Such potential demands studying how RPA can accurately and automatically provide the important FR monitoring parameters mentioned by McDonald et al. [7], such as tree cover, tree density, and tree species. In biomes like the Brazilian Atlantic Forest, which is a biodiversity hotspot [8], improving the FR monitoring protocol would help managing the targets stipulated under the Paris Agreement, wherein Brazil is committed to restoring 12 million hectares of forests by 2030.

This study aims to evaluate the manner in which RPA can contribute to the FR monitoring protocol of the Brazilian Atlantic Forest. Particularly, we evaluated a low-cost RPA [9] because financial resources are scarce in developing countries [10]. These findings play an important role in improving the FR monitoring protocol by considering an emerging remote sensing technology.

2. Materials and Methods

2.1. Study Area

The FR study area is located in the Brazilian Atlantic Forest biome, specifically at the Miguel Pereira Municipality in the state of Rio de Janeiro (RJ). Figure 1 illustrates this 23.45 hectare study area, where Instituto Terra de Preservação Ambiental (ITPA) conducted an FR project.

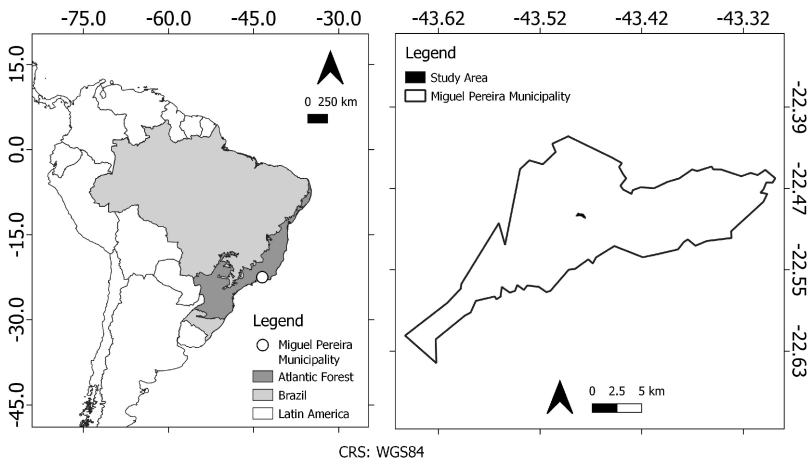

Figure 1. Location of the FR study area on Miguel Pereira municipality, situated in the Brazilian Atlantic Forest biome. To see the RPA orthomosaic and the study area on a greater scale, please go to Figure 3.

The traditional fieldwork with 19 field plots to officially monitor the FR occurred in October 2017. It followed the Fast Environmental Diagnosis Methodology [11], which is

Rio de Janeiro State's official FR monitoring process. In January 2018, the RPA fieldwork was conducted in the study area.

2.2. Materials

The RPA used in this study is a Phantom 4 Standard (a rotary wing). It is coupled with an RGB 1/2.3" 12MP camera with FOV 94° 20 mm (35 mm format equivalent) lens, Electronic Shutter Speed of 8–1/8000 s, and Image Size of 4000 × 3000. More information regarding this RPA model can be found at https://www.dji.com/br/phantom-4, accessed on 26 May 2021.

The flight plan was drafted using the free software Pix4D Capture for smartphones/tablets. The Digital Surface Model (DSM) and orthorectified mosaic were obtained using the Agisoft Photoscan software. The classification processes and graph generation were performed using R [12] version 3.6 and the map layouts were generated using QGIS software version 3.12. The Cloud Compare software was used to generate the Digital Terrain Model (DTM).

2.3. Methods

2.3.1. Flight Patterns

Two flights were necessary to cover the entire study area. The flights were conducted in compliance with Brazil's RPAs laws [13] at a height of 80 m and generated an 8 cm Ground Sampling Distance (GSD). The front and side overlaps were equal to 80% to generate enough details in the point cloud data [14].

No Ground Control Points (GCPs) were collected by a geodetic Global Navigation Satellite System (GNSS) equipment, and thus the orthomosaic precision was around 3 m [15]. Such cartographic precision is considered enough for this study because change detection over time was not performed in this study [16].

2.3.2. Estimation of Forest Restoration Biodiversity Using Low-Cost RPA

Tree species were not distinguishable by photointerpretation on the RPA orthomosaic, as illustrated in Section 3. Thus, the estimation of the FR parameter Biodiversity by low-cost RPA was not considered in this study. Instead, this study focused on the FR structural parameters, which play an important role in FR monitoring [7]. The remotely measured FR structural parameters were Tree Density, Vegetation Cover, Tree Height, and Grass Infestation. Figure 2 shows the workflow for obtaining these FR structural parameters and the accuracy assessment. Sections 2.3.3–2.3.7 describe each step presented in Figure 2.

2.3.3. FR Structural Parameter: Tree Density

To estimate the Tree Density parameter, individual trees must be counted. Some studies have counted trees automatically using the Canopy Height Model (CHM) database [17], as the CHM is the difference between the DSM and the DTM [18]. In this work, the DTM was created by applying the Cloth Simulation Filter algorithm [19] in Cloud Compare software. Since the study area was sloping and contained some small trees, which were slightly higher than the grasses, these short trees were omitted in the DTM generation, and the CHM was consequently affected. Thus, the individual tree count was obtained directly from the DSM to increase automatic tree counting accuracy, as described in Albuquerque et al. [14].

The Local Maximum algorithm [20,21] of the rLiDAR R package [21] was used on the DSM to obtain the individual tree count. This algorithm searches for the highest value on a fixed window-sized kernel and generates a point table with geographic coordinates of the encountered maximum values. Individual tree count is then obtained by a coordinate set, where each coordinate represents the highest location of a tree crown.

To avoid the individual tree count commission errors (false-positives), two or more coordinates with a distance of less than 10 cm between them were excluded because they represent the same tree. Then, the geographic coordinates of the point halfway between these excluded points were retained to represent the tree. The ten-centimeter threshold

value was defined because forest inventories consider only trees with trunk diameters of >5 cm [22], and thus trees must be at a distance of at least 10 cm from each other. More details about the individual tree count method applied in this work can be found in [14].

After the individual tree count was determined, the number of identified trees was divided by 23.45 hectares (size of the study area) to obtain the tree density.

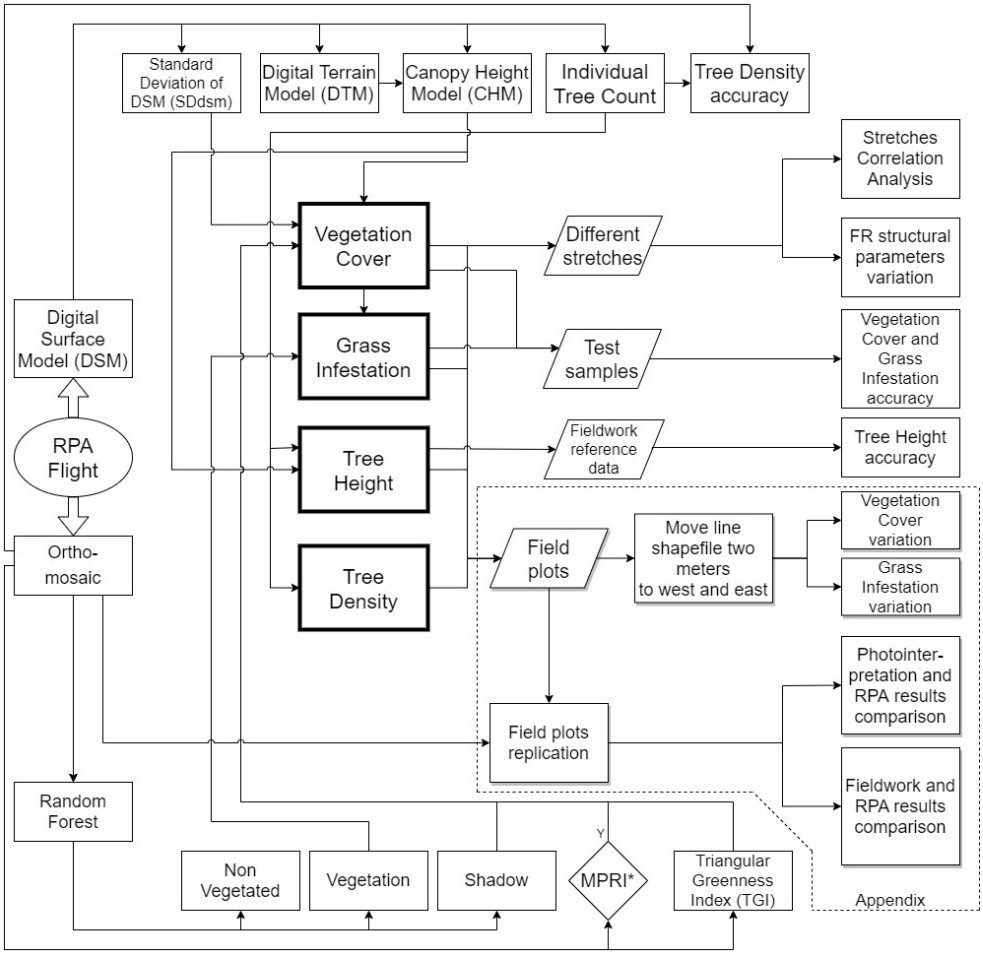

Figure 2. Methodology workflow of this study. MPRI is the Modified Photochemical Reflectance Index [23] and should be used only in the absence of shadow.

2.3.4. FR Structural Parameter: Tree Height

Tree height was determined in two steps: (1) extracting the CHM value corresponding to each geographic coordinate in the individual tree count; (2) calculating the mean of these extracted values. The height values were obtained from the individual tree count results as they correspond to the largest tree crown height value.

2.3.5. FR Structural Parameter: Vegetation Cover

To determine vegetation cover using RPA imagery, trees and grasses must be adequately distinguished. Vegetation cover involves the area covered by trees and not by grass, as Grass Infestation is a FR structural parameter described in Section 2.3.6. This study therefore considers that the variable vegetation is the sum of Vegetation Cover and Grass Infestation.

$$Vegetation = VegetationCover + GrassInfestation \quad (1)$$

Vegetation mapping was performed using a Random Forest supervised classification involving three land cover classes according to Reis et al. [24] and Laliberte et al. [25]: vegetation, shadow, and non-vegetated.

When using RPA to determine the vegetation cover, the CHM should involve only areas with trees, and therefore an accurate CHM would by itself provide the Vegetation Cover parameter. As explained in Section 2.3.3, trees that were slightly higher than grasses on sloping areas were excluded during CHM acquisition, and thus this database could not be used by itself to accurately obtain Vegetation Cover. To isolate Vegetation Cover, vegetation indexes like the Triangular Greenness Index (TGI) (Equation (2)) [26] can be an alternative.

$$TGI = [(Green - 0,39) * (Red - 0,61)] * Blue \quad (2)$$

TGI is not a normalized index, and vegetated areas tend to present negative values. In this work, the TGI could distinguish between trees and grasses, but it did not provide a final Vegetation Cover result on its own because some trees or some parts of tree crowns were missing, and thus the Standard Deviation of DSM (SDdsm) was also used for Vegetation Cover mapping.

The Standard Deviation of DSM (SDdsm) may be used to avoid confusion between trees and grasses because it has presented good results in detecting homogeneous topographic surfaces [27] and the arboreal stratum [28]. However, in medium-aged FR projects, like the one in this study, the height of trees varies considerably, and thus the application of SDdsm for vegetation cover mapping presents some limitations and should be used along with other variables.

Thus, the Vegetation Cover result acquired by RPA in this study was the sum of TGI Vegetated areas (TGIVeg), Standard Deviation of DSM (SDdsm), and CHM. As indicated by Equation (3), the sum of these variables for the Vegetation Cover mapping also involved the exclusion of shaded areas.

$$VegetationCover = [(TGIVeg + SDdsm + CHM) - (3 * Shadow) > 0] \quad (3)$$

Each variable in Equation (3) is a raster containing values equal to zero (means no occurrence) or one (means occurrence). Furthermore, in Equation (3), it is noteworthy that shaded areas, obtained by the land cover class Shadow, are multiplied by the number of layers containing vegetation areas. This ensures that areas mapped as vegetation by more than one vegetation layer will receive zero or negative values when they are overlapping with shaded areas. Moreover, if the values of the variables in Equation (3) are selected to be greater than zero, the equation can be solved using one line of computation code, instead of two.

Regarding the Modified Photochemical Reflectance Index (MPRI) [23], it did not contribute to Vegetation Cover mapping in this work because it generated a large amount of confusion with shaded areas.

2.3.6. FR Structural Parameter: Grass Infestation

In reality, Grass Infestation may overlap with Vegetation Cover because grass grows below a tree crown. However, Structure from Motion and Multi-View-Stereo [29,30], or SfM-MVS, is unable to record the surface below the tree crowns, and thus, in this study, it is considered that Grass Infestation does not overlap with Vegetation Cover.

Therefore, Grass Infestation mapping was conducted using Equation (1), which led to Equation (4) because Section 2.3.5 describes Vegetation and Vegetation Cover acquisition.

$$GrassInfestation = Vegetation - VegetationCover \quad (4)$$

2.3.7. Accuracy Evaluation

Remote measurements in environmental projects must be conservative, which means that overly optimistic results must be avoided [31]. Regarding the Grass Infestation struc-

tural parameter, as it is an undesirable variable in the Brazilian Atlantic Forest biome, an estimation containing more commission than omission errors is considered conservative. For Vegetation Cover, Tree Height, and Tree Density, which are desirable variables, the conservative path involves more omission than commission errors. In other words, FR classification results obtained using remote sensing must avoid commission errors in desirable FR structural parameters and avoid omission errors in undesirable FR structural parameters.

To estimate Tree Density in closed-canopy conditions, fieldwork may be necessary for acquiring reference data because the boundaries of the overlapping tree crowns may not be clearly identifiable by photointerpretation [32,33]. Since the canopy was not closed in the study area, a photointerpretation qualitative analysis [34] evaluated the accuracy of Tree Density. This qualitative analysis allowed the acquisition of omission and commission errors, or the amount of False-Positive (FP) and False-Negative (FN) occurrences, as well as the Overall Accuracy [35]. Recall, Precision, and F_score indexes [36] were then calculated according to Equations (5)–(7), respectively.

$$r = \frac{TP}{(TP + FN)} \tag{5}$$

$$p = \frac{TP}{(TP + FP)} \tag{6}$$

$$F_{score} = 2 * \frac{(r * p)}{(r + p)} \tag{7}$$

where: TP = True Positive, FN = False Negative, FP = False Positive, r = recall, p = precision.

Vegetation Cover and Grass Infestation accuracies were measured using a Confusion Matrix, along with Overall Accuracy, Producer's Accuracy, User's Accuracy, F_score, and Kappa Index. In total, 50 test samples were used for each of the three classes: Vegetation Cover, Grass Infestation, and Other Classes.

Tree Height is the only FR structural parameter in this study that cannot be evaluated by photointerpretation. Therefore, the accuracy of this parameter was measured using the Error Percentage [37] between the fieldwork and RPA results (Equation (8)).

$$ErrorPercentage = \frac{(Reference - Results)}{(Reference)} \tag{8}$$

2.3.8. Evaluating FR Structural Parameters Values in Stretches with Different FR Success

Since RPA can be used to map the entire project area, stretches with different vegetation singularities can be noticed [38]. In that case, stretches with more, less and intermediate FR success within the study area were manually separated by photointerpretation. The intermediate FR success stretches in this work were a mix of more and less FR successful areas. Figure 3 illustrates the polygons that represent these stretches.

A boxplot and correlation matrix quantitatively indicated if the different stretches in Figure 3 have different FR structural parameters. The boxplot illustrated how the FR structural parameters values vary between the final fieldwork results (the final fieldwork results can be found in Appendix A.3), as shown by Equation (9).

$$ErrorPercentage_{stretch} = \frac{(Fieldwork - RPA_{stretch})}{(Fieldwork)} \tag{9}$$

Thus, for each FR structural parameter, a boxplot graph was used to evaluate how the Error Percentage (Equation (9)) varied among the different FR stretches.

Furthermore, for example, to assess whether a high value of Vegetation Cover is associated with low values of Grass Infestation (it is expected that grass reduces as the canopy closes), a correlation matrix of the RPA results in the different stretches was evaluated.

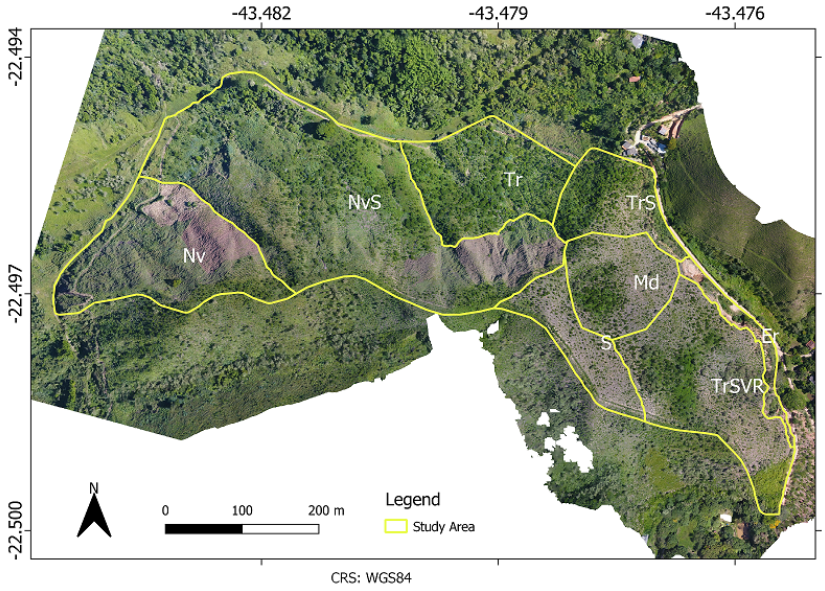

Figure 3. Study area divided into 8 different stretches with more, less, and mixed quantities of forested areas (FR success): Non-vegetated predominance (Nv), Non-vegetated mixed with Seedlings (NvS), Trees predominance (Tr), Trees mixed with Seedlings (TrS), Seedlings predominance (S), Trees mixed with Seedlings mixed with Vegetation Remnants (TrSVR), Erosions (Er) and Model (Md). The Md stretch was the one that best represented the whole study area in general.

3. Results

Regarding the Biodiversity parameter, it was not possible to identify tree species when replicating field plots in the RPA image. As shown in Figure 4, the study area has different tree species that presented similar spectral responses in the visible spectrum and similar geometric forms in the RPA image, which makes the classification process not possible because the human eye cannot state the difference [39]. Thus, traditional fieldwork will continue being necessary to record tree species in FR projects, and future studies should evaluate the performance of other types of sensors, such as multispectral and hyperspectral, in the estimation of Biodiversity.

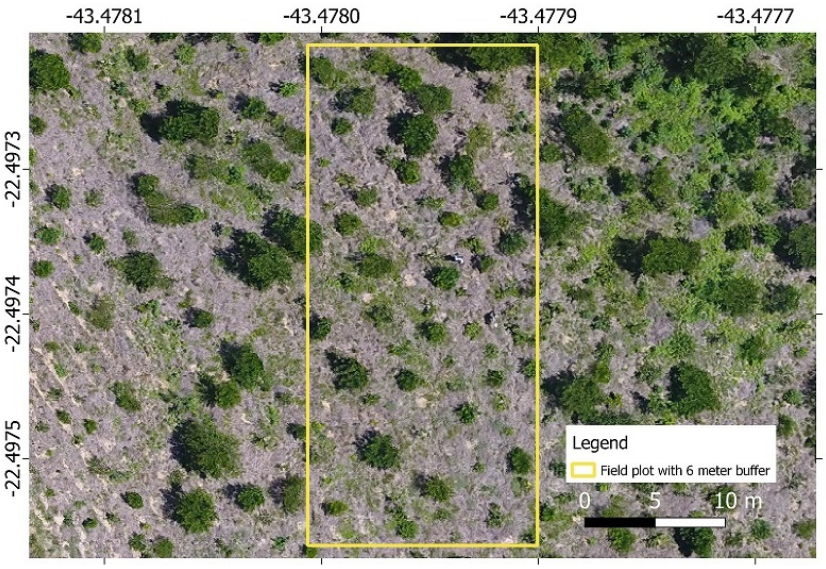

Figure 4. There are at least six different tree species in the rectangle area, but all of them are very similar, and none could be distinguished by photointerpretation.

Regarding the FR structural parameters, which were the focus of this study, Figures 5–7 show the RPA results in the whole study area. Figure 8 shows a zoomed-in version of the RPA results in the study area.

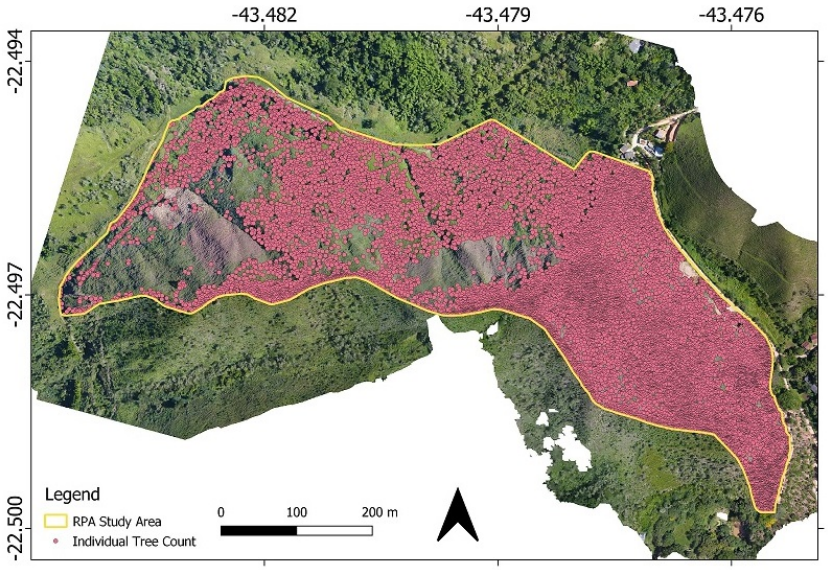

Figure 5. Individual Tree Count results of the RPA study area, which provided the Tree Density result when dividing all the identified trees by the area.

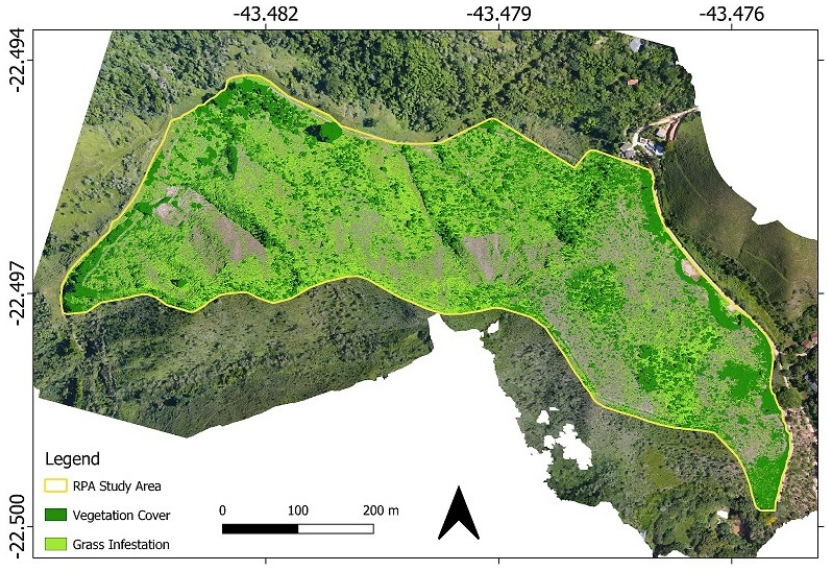

Figure 6. The Vegetation Cover and Grass Infestation results of the RPA study area.

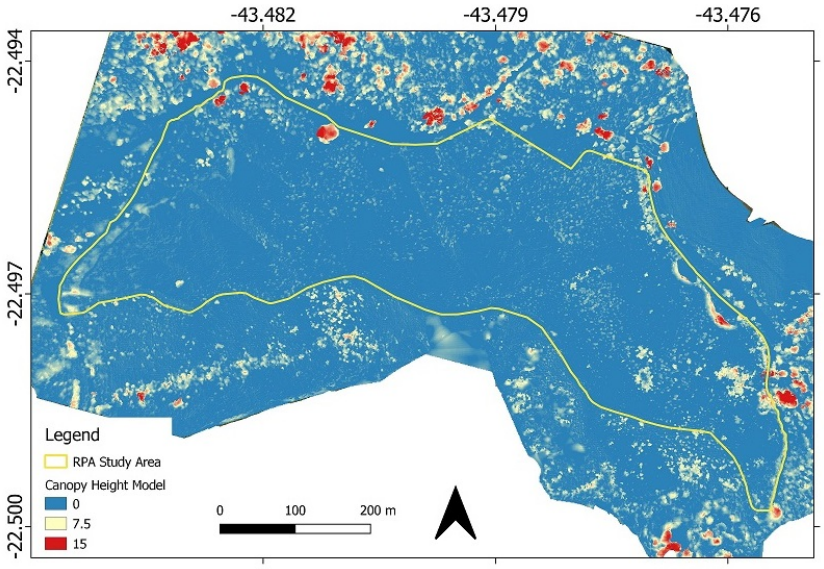

Figure 7. The Canopy Height Model (CHM) results of the RPA study area, which provided the height of the trees that were automatically identified. The zero CHM values mean grasses or non-vegetated (bare soil) areas.

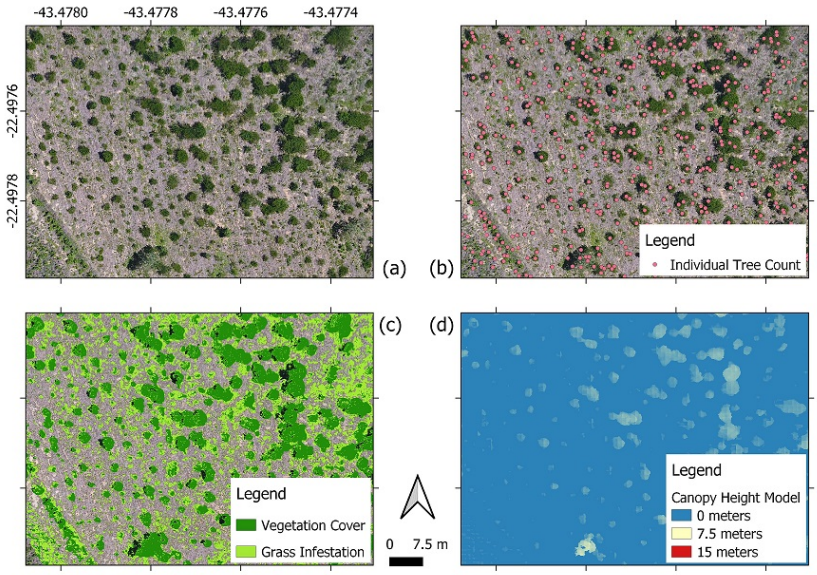

Figure 8. FR structural parameters results of the study area in a high mapping scale. (**a**) The RPA orthomosaic. (**b**) The Individual Tree Count, which provided the Tree Density result when dividing all the identified trees by the area. (**c**) The Vegetation Cover and Grass Infestation results. (**d**) The Canopy Height Model (CHM), which provided the height of the trees that were automatically identified and where zero CHM values means grasses or bare soil areas.

3.1. Vegetation Cover and Grass Infestation Accuracy

The Confusion Matrix shown in Table 1 presents high accuracy indexes for Vegetation Cover and medium accuracy indexes for Grass Infestation. The Overall Accuracy and the Kappa index of the Confusion Matrix are equal to 0.75 and 0.63, respectively. The F_score value was equal to 0.85 and 0.64 for Vegetation Cover and Grass Infestation, respectively. F_score ranges from 0 to 1 and has been widely used [14,17,32,33,40–44], and thus 0.85 and 0.64 can be considered high and medium accuracy values, respectively.

Table 1. Confusion Matrix for measuring Vegetation Cover (Trees) and Grass Infestation (Grass) accuracy.

		Target				
		Grass	**Trees**	**Other Classes**	**Producer's Accuracy**	**User's Accuracy**
Prediction	**Grass**	26 (52%)	5 (10%)	0 (0%)	52%	84%
	Trees	1 (2%)	41 (82%)	4 (8%)	82%	89%
	Other Classes	23 (46%)	4 (8%)	46 (92%)	92%	63%

3.2. Tree Density Accuracy

The Individual Tree Count method to obtain Tree Density presented Recall, Precision, F_score, and Overall Accuracy values equal to 0.93, 0.90, 0.92, and 0.87, respectively. These are considered high accuracy results. However, Individual Tree Count presented 10% of commission errors (undesirable for Tree Density), which may have influenced the achievement of accurate results because omission errors were compensated.

3.3. Tree Height Accuracy

The Tree Height value was equal to 1.68 m and 1.93 m when obtained using RPA and fieldwork (reference data), respectively. With such results, the Error Percentage was equal to 0.13, and thus Tree Height was accurate when measured by RPA because it is a conservative result that estimates a 13% shorter height for trees that are almost 2 m tall.

3.4. FR Structural Parameters Values in Stretches with Different FR Success

The stretches with different FR success, described in Section 2.3.8, presented some variation in the RPA results. As Figure 9 shows, only Vegetation Cover presented small variation among the different stretches, suggesting the presence of small tree crowns in general because Tree Density varied more considerably. Furthermore, some variations in Tree Height, Tree Density and Grass Infestation reinforce the occurrence of different FR success that were indicated by photointerpretation.

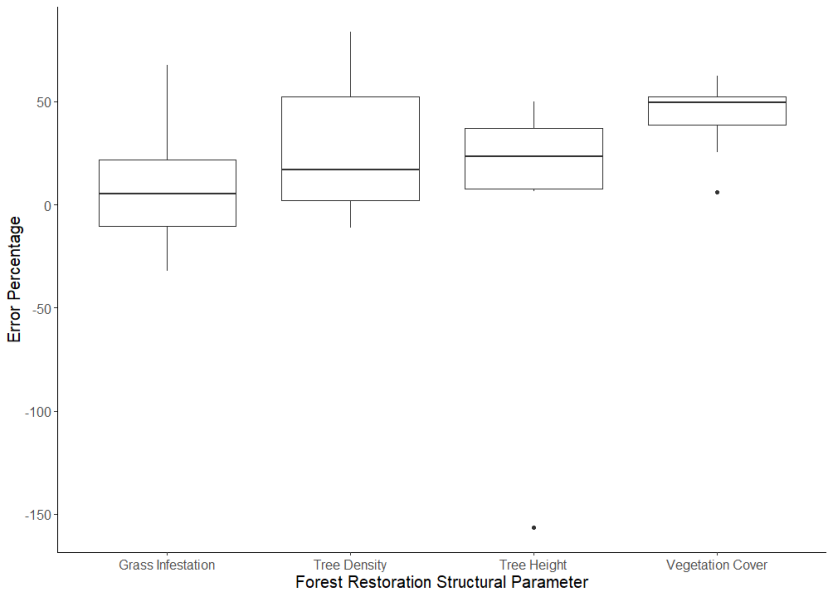

Figure 9. FR structural parameters of the stretches with different FR success varied from the fieldwork reference value, except Vegetation Cover. A variation in Tree Density and non-variation of Vegetation Cover suggest small tree crowns in general.

Figure 10 shows that the FR structural parameters presented some correlation between them. Such correlation suggests some ecological succession process: Grass Infestation has a high negative correlation with the development of trees; the taller the trees, the bigger the tree crowns (high correlation between Tree Height and Vegetation Cover); and many trees presented small tree crowns (medium correlation between Tree Density and Vegetation Cover).

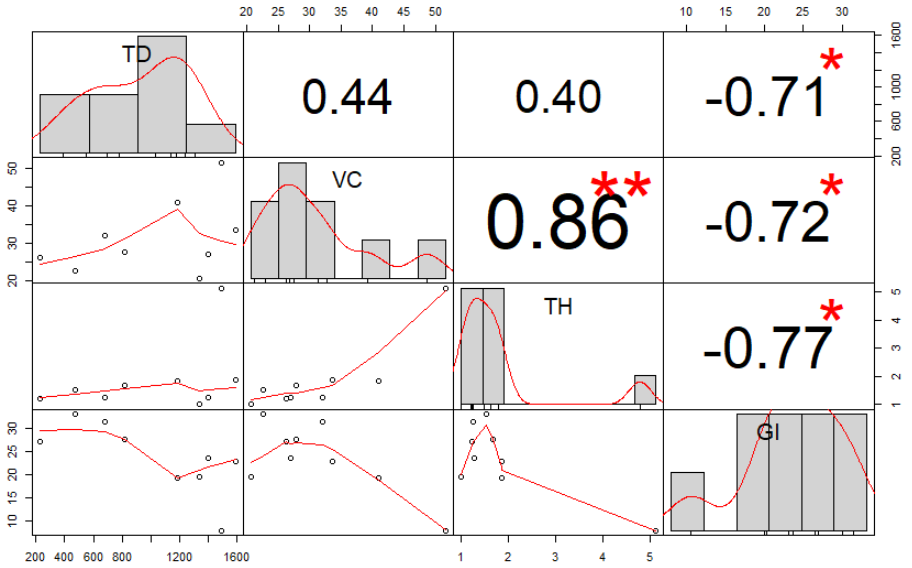

Figure 10. FR structural parameters Correlation Matrix between different FR stretches. In this symmetric matrix, the cells of the main diagonal shows a FR structural parameter (TD is Tree Density, VC is Vegetation Cover, TH is Tree Height, and GI is Grass Infestation) and its corresponding values in the different FR stretches. The other cells show the correlation value between different FR structural parameters, where the more asterisk ("*") symbol occurs, the more correlated two variables are.

4. Discussion: Lessons Learned

In this study, we present the Discussion section as lessons that were learned, and thus each lesson is presented as a subsection. The subsection title represents the lesson itself, while the corresponding text complements and discusses it. By highlighting each lesson as a subsection, we intend to make its discussion easier to be found in the manuscript.

4.1. Low-Cost RPA Is Capable of Accurately Mapping Forest Restoration (FR) Structural Parameters in Open Canopy Conditions

Although previous works accurately evaluated tree cover and tree height using low-cost RPA [44–46], this study evaluated four structural parameters (Vegetation Cover, Tree Height, Tree Density and Grass Infestation) in the context of FR and in a sloping area, which represents a common situation in the Brazilian Atlantic Forest Biome.

RPA works at the local scale only [47], but if a regional scale is desired, the Landsat satellite, although having a lower spatial resolution when compared to other remote sensing databases, showed potential for monitoring the vegetation expansion of FR projects throughout the years [48]. Still regarding FR monitoring at the regional scale, initiatives like the MapBiomas project (https://mapbiomas.org/, accessed on 15 June 2021) show the locations of secondary forests for free.

The Landsat free available satellite imagery may provide valuable information, but its spatial resolution generates inconsistencies when more refined data is needed to evaluate the FR [47]. Thus, each technology has advantages and disadvantages, and this work reinforces that low-cost RPA is a good alternative for collecting data to monitor the FR at the local level. Since low-cost RPA is capable of accurately mapping FR structural

parameters in open canopy conditions, future studies shall evaluate FR areas with closed-canopy conditions.

4.2. To Improve the Accuracy of the Tree Height Measurement by Low-Cost RPA in All the FR Stages, a Possible but Expensive Solution would be Using Precise Global Navigation Satellite System (GNSS) Data

Although the Tree Height was accurate in this work, the CHM omitted trees that were slightly higher than grasses in the sloping area. To handle this situation, a flight prior to the tree growth using precise GNSS coordinates could obtain an accurate (or a literal) DTM. Then, after the FR process begins (after trees begin to grow), an accurate CHM would be possible due to a refined DTM availability for the future RPA data acquisition, which would also demand precise GNSS coordinates.

Besides checking if a precise DTM would include small trees in the CHM of sloping FR areas, the use of precise GNSS data would also confirm if the accuracy of the tree height measured using SfM-MVS increases even when the canopy closes. The use of traditional topography methods (when geodetic GNSS equipment and total station are required) generates a refined DTM in closed-canopy conditions, which allows accurate Tree Height measurements via SfM-MVS [49]. However, classic topography increases the costs of the projects due to the time spent in the field [50] and to the costs of the equipment [51], and thus the benefits of using ground control points for Tree Height measurement via RPA data collected before and after the tree growth must be carefully studied in the future.

To avoid collecting precise GNSS data on every RPA flight for the Tree Height measurement, survey markers can be installed on the FR surroundings, and thus the precise geographic coordinates can be collected only once. After collecting the precise GNSS coordinates, the survey markers can become ground control points (GCP) for the RPA data by putting visual targets above them before each RPA flight. The location of the survey markers has to be the FR surroundings because they must be visible on the RPA data after the canopy closes.

Alternatively, to avoid using survey markers or precise GNSS coordinates on every SfM-MVS cartographic data, collecting different RPA images of the same area along the FR evolution could enable an independent analysis of each orthomosaic until the canopy closes. Future studies may confirm if precise GNSS coordinates are necessary only for a precise DTM generation (when trees have not started to grow) and for the RPA images acquired after the canopy closes.

Tree Height is a relevant structural parameter because it is related to ecology [52], biomass [49,53], and biodiversity [53,54], and measuring it in closed-canopy conditions is not an issue in LiDAR systems [46,53,55]. However, LiDAR systems are considered more expensive, which is not ideal for the financial reality of developing countries [10]. Thus, more studies of Tree Height measurement by SfM-MVS in closed-canopy conditions must be conducted. Tree Height measured by RPA is a field of research that may benefit not only the FR and mature forests, but also different commercial plantations and crops [56].

4.3. Via Photointerpretation, RPA Can Identify Stretches with Different FR Success That Present Different Values of FR Structural Parameters

One of the advantages of RPA is that the entire FR area can be measured, and thus stretches with different degrees of FR success were visually identified. The values of the FR structural parameters in these stretches presented some variation from the fieldwork reference value, as indicated by the standard deviation of the boxplots shown in Figure 9.

Although the RPA has the advantage of identifying stretches with different FR success, such benefit occurs at the local scale only. If a regional FR monitoring scale is required, Landsat images, due to its spatial resolution, have the potential to identify only considerable increases in vegetation cover [48].

The possibility of identifying stretches with different FR success via photointerpretation of the low-cost RPA orthomosaic reinforces another advantage of monitoring FR using high spatial resolution images: it provides valuable information in open-canopy conditions

even if no more data of the FR site, like field plots, is available. Since photointerpretation of low-cost RPA orthomosaic generates reference data for Tree Cover, Tree Density and Grass Infestation, which are relevant structural parameters, managers can check stretches with less FR success that may need some intervention using RPA data only.

Besides being capable of identifying stretches with different FR success, the FR structural parameters evaluated in this study were based on the Rio de Janeiro local environmental agency [11], and Tree Height was the only FR structural parameter that demanded a traditional fieldwork for reference data acquisition in open canopy conditions. Traditional fieldworks are necessary to evaluate the computational 3D modeling because it is not possible to check tree heights using a photointerpretation of the CHM. Even LiDAR systems that accurately measured Tree Height demanded traditional fieldwork for acquiring reference data [46,53,55]. Thus, Tree Height is the only FR structural parameter evaluated in this study that demands fieldwork to assess its remote sensing accuracy, which reinforces that low-cost RPA data register valuable information for FR projects even if no field plot data is available.

4.4. RGB Limitations for Identifying Different Tree Species Reinforced That Biodiversity and Remote Sensing Constitute a Specific Field of Research and That Traditional Fieldwork Will Continue Being Necessary in the Future

Although modern Computer Vision techniques, such as Deep Learning, have demonstrated that low-cost RPA can be used to identify palm species in the Amazon [32] or tree species in a German forest [33], it is still not possible to handle the biodiversity of Brazilian FR projects solely via high-resolution RGB imagery. The tree species of the Atlantic Forest Biome in this study looked very similar in the RPA imagery, but since the Biodiversity parameter is relevant for FR projects, future works must check if other species, which were not present in the study area, are distinguishable in high-resolution RGB images. These future studies must generate two databases with precise Global Navigation Satellite Systems (GNSS) geographic coordinates: the low-cost RPA data, which must present ground control points to improve its cartographic precision (1); and the tree species location, which must be a layer where each tree has a precise geographic coordinate associated with its corresponding species. These two databases will make it possible to verify which tree species are distinguishable via photointerpretation.

In this work, even if the two databases mentioned in the previous paragraph (RPA data and tree species location with precise GNSS coordinates) were available, the Biodiversity parameter would still not be possible to be measured via low-cost RPA because photointerpretation could not distinguish different tree species. After all, the targets in the images must be visually distinguishable for a proper reference data [35,39]. A possible solution for this low-cost RPA limitation for recognizing different species may be the flowers of the trees. The flowers can make some tree species distinguishable via photointerpretation, but the remote sensing data must be collected in the flowering period [42], which reinforces the challenge involving Biodiversity and remote sensing.

Another alternative for measuring the Biodiversity parameter via remote sensing would be an estimation of the number of species in a FR site instead of the identification of the species of each tree. When dealing with the number of species, an unsupervised classification could be applied, but reference data would still be necessary [35,57]. In this study, as previously mentioned, there was no reliable Biodiversity reference data for remote sensing estimations due to a significant similarity between the different tree species in the RPA imagery.

Almeida et al. [53] used a refined remote sensing dataset provided by a LiDAR system and also mentioned a biodiversity challenge in the Atlantic Forest Biome because the authors accurately measured canopy structure and above-ground biomass of FR areas, but not species richness. Alonzo et al. [58] used LiDAR and hyperspectral sensors to map 29 tree species considering 30 different remote sensing classes: 29 classes corresponded to 29 different tree species, while 1 class involved different and non-frequent tree species. Thus, regarding the biodiversity challenge, even if multispectral, hyperspectral, or LiDAR sensors

prove to be capable of automatically identifying tropical rainforest species in the near future, the costs of such sensors must decrease considerably if a practical FR monitoring protocol is desired. Traditional fieldwork will therefore continue being necessary and remote sensing may be applied using applications onboard smartphones and tablets, like Agrotag [59], for monitoring the FR biodiversity.

Applications onboard smartphones and tablets like Agrotag can take pictures at the ground level of the tree species and can also share the FR monitoring data collected by field plots on an online Geographic Information System (GIS) platform. Future studies may evaluate if using a low-cost RPA for measuring the structural parameters and an application onboard smartphones and tablets for measuring the Biodiversity parameters are capable of accurately providing a full FR monitoring report.

5. Conclusions

For the development of a practical FR monitoring protocol, low-cost RPA was found to be accurate for the measurement of the FR structural parameters. Only Grass Infestation, which is the least important indicator, presented medium accuracy. In addition to improving the accuracy of the Grass Infestation parameter, future studies must evaluate the optimal remote sensing techniques for FR projects of different ages, with a particular focus on how low-cost RPA can accurately measure the FR structural parameters when the canopy is closed. After all, each FR stage will require different remote sensing techniques.

Although low-cost RPA can accurately measure the structural parameters, it cannot accurately measure the FR biodiversity parameter in the Brazilian Atlantic Forest, and thus traditional fieldwork will continue being necessary. It may be possible to utilize an RPA and then use field plots for biodiversity monitoring only, but this would require FR consultants and environmental agencies to evaluate the costs of adding a remote sensing professional to their teams.

Author Contributions: Conceptualization, R.W.A., M.E.F., C.P.B., M.R.C.B. and C.H.G.; methodology, R.W.A.; software, R.W.A. and C.H.G.; validation, R.W.A., M.E.F., S.I.O. and C.H.G.; formal analysis, R.W.A., M.E.F. and C.H.G.; investigation, R.W.A., H.M. and J.V.S.C.; resources, R.W.A., M.E.F., H.M., J.V.S.C. and C.H.G.; data curation, R.W.A. and C.J.R.M.; writing—original draft preparation, R.W.A.; writing—review and editing, R.W.A., M.E.F., S.I.O., C.J.R.M. and C.H.G.; visualization, R.W.A., M.E.F., S.I.O., C.J.R.M. and C.H.G.; supervision, R.W.A. and C.H.G.; project administration, R.W.A., M.E.F., J.R.C.T. and C.P.B.; funding acquisition, J.R.C.T., C.P.B. and C.H.G. All authors have read and agreed to the published version of the manuscript.

Funding: This study was financed in part by The Nature Conservancy Brazil (TNC) and in part by the Coordenação de Aperfeiçoamento de Pessoal de Nível Superior—Brasil (CAPES)—Finance Code 001. M.E.F. (grant #315699/2020-5) and C.H.G. (grant #423481/2018-5 and #304413/2018-6) are CNPq Research Fellows. The APC was funded in part by The Nature Conservancy Brazil (TNC) and in part by the Coordenação de Aperfeiçoamento de Pessoal de Nível Superior—Brasil (CAPES)—Finance Code 001 of the Programa de Pós-Graduação em Ciência Ambiental (PROCAM) from University of São Paulo (USP).

Acknowledgments: The authors thank The Nature Conservancy Brazil (TNC), the field support of Instituto Terra de Preservação Ambiental (ITPA), Laboratório de Engenharia Cartográfica (LECAR) from Universidade Estadual do Rio de Janeiro (UERJ) and the Federal University of Goiás/LAPIG/ProVant for the provision of RPA equipment. We also thank the SPAMLab at IEE-USP for data processing and analysis infrastructure. We are thankful to the landowners of the forest restoration areas (ITPA's partners) for authorizing our access and to Instituto Estadual do Ambiente (INEA) for the FED methodology results grant.

Conflicts of Interest: The authors declare no conflict of interest. The funders had no role in the design of the study; in the collection, analyses, or interpretation of data; in the writing of the manuscript, or in the decision to publish the results.

Appendix A. Field Plot Replication in RPA Imagery

Appendix A.1. Methods: Field Plot Replication in RPA Imagery

As mentioned in Section 2.3.2, a field plot replication in the RPA image was initially motivated to study the Biodiversity parameter, but since all trees were very similar in the RPA image, an evaluation of the FR structural parameters inside the polygons that represent the field plots was conducted.

The rectangle shapefiles that represented the 25 × 4 m field plots were generated like the fieldwork procedures, where the field plots coordinates correspond to the southernmost latitude and middle longitude of the field plot rectangles. From these coordinates, 25 m lines were generated with 0° Azimuth. The field plot rectangle is then completed by considering 2 m from each perpendicular direction of the 25 m line, forming a 25 × 4 m plot rectangle [11]. Figures A1 and A2 illustrates examples of this field plot rectangle procedure.

When analyzing the RPA results inside the field plot rectangles, two different reference data were considered due to the cartographic uncertainty of the orthomosaic and of the field plot location. These two reference data were the photointerpretation of the field plot rectangles (photointerpretation has no cartographic uncertainty with the RPA results because both came from the same database) and the fieldwork data of each field plot. The differences between the RPA accuracy results considering these two reference data were then recorded and analyzed. The accuracy measurement unit is described in Appendix A.2.

When generating the photointerpretation of the field plots rectangles as Figure A2 shows, the authors stated that the position of the 25-m line considerably influences Vegetation Cover and Grass Infestation parameters. To quantitatively measure such an influence, an experiment was conducted where Vegetation Cover and Grass Infestation were measured in different positions over the RPA image, as explained in the next paragraphs.

In traditional fieldwork, Vegetation Cover is obtained by stretching a 25 m measuring tape on the floor. The length of the measuring tape covered by trees is noted and then divided by 25 m. If, for example, the number of meters covered by trees is 25 or 12.5, you get 100% and 50% of Vegetation Cover, respectively. Figure A1 illustrates the fieldwork procedures for the Vegetation Cover measuring procedure.

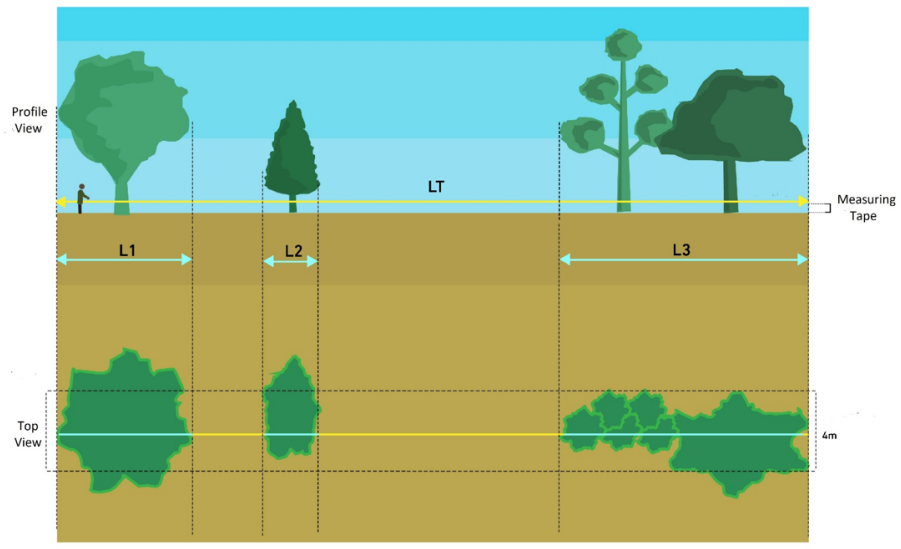

Figure A1. Vegetation Cover measuring procedure on a 25 × 4 m plot, where LT is Linear Totality. In the fieldwork procedures, LT is equal to 25 m, and the field plot is defined by considering 2 m from each LT perpendicular direction, forming then a 25 × 4 m plot. L1, L2, and L3 are examples of linear measurements in LT that are covered by trees. Thus, Vegetation Cover is the sum of L1, L2, and L3 divided by LT. Source: adapted from INEA [11].

When applied to RPA imagery, this method can be subject to some issues because Vegetation Cover is an area measurement (two dimensions), and the measuring tape measures lengths (one dimension). As can be seen by Figure A1, if the measuring tape moves 2 m to the left or the right in an RPA image, the Vegetation Cover parameter may considerably vary.

To verify if moving the measuring tape 2 m to the left or the right considerably affects Vegetation Cover on RPA imagery, an experiment was conducted. In such an experiment, the amount of line that covered trees was verified by photointerpretation in three different positions for each field plot. In the first position, the 25-m line is in the field plot coordinate (which is the position for measuring Vegetation Cover according to the fieldwork procedures). In the second and third positions, the line shifted 2 m to the left (west direction) and 2 m to the right (east direction). After verifying the amount of tree cover on these positions, the variation (between the first position and the other two positions) was noted in percentage. Regarding the 2 m value, it represents an usual imprecision value of a common GNSS equipment [60], and it is also the value that the fieldwork procedures move (to the left and the right) to generate a 25 × 4 m plot. Figure A2 illustrates this 2-m shifting process evaluation.

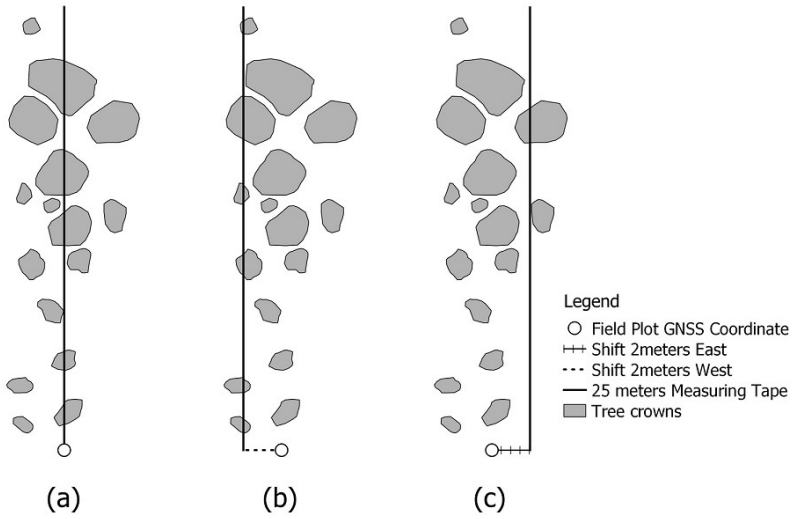

Figure A2. An experiment to quantitatively measure the influence of the measuring tape position in Vegetation Cover acquisition if trying to replicate the fieldwork procedures on RPA imagery. Vegetation Cover value from the middle longitude of the field plot, which is where the measuring tape is positioned in the fieldwork procedures, (**a**) was compared to the Vegetation Cover value when moving the measuring tape 2 m in the west direction (**b**) and the east direction (**c**).

If this experiment, illustrated in Figure A2, confirms that Vegetation Cover considerably varies when moving the line shapefile, remote sensing may be reinforced as an alternative to improve this variable measurement. It would also verify that replicating traditional fieldwork procedures over RPA images is not a good idea.

Such an experiment of moving the measuring tape 2 m to the right and the left was also made for Grass Infestation because it has the same Vegetation Cover fieldwork procedures that are illustrated in Figure A1.

It must be mentioned that when comparing RPA and fieldwork results, some issues found that the overflown study area did not involve the whole area monitored by fieldwork results. Overall, 19 out of 28 field plots, which corresponds to 23.45 out of 28.55 hectares of the FR area, were covered by the RPA imagery, while Vegetation Cover and Grass Infestation fieldwork values were not recorded for each field plot (only the final value was recorded). This means that 17.8%$((28.55 - 23.45)/28.55 = 0.178)$ of the area monitored by fieldwork procedures, and not by RPA imagery, contained 32% of the field plots. Regarding those not overflown field plots, Google Earth's free available imagery showed by photoint-

erpretation that these were the FR areas with the highest tree cover (canopy was almost closed), which could also suggest the highest values of other FR structural parameters.

Appendix A.2. FR Structural Parameters Accuracy Evaluation Inside Field Plots

When replicating the FR structural parameters inside the field plots, it is expected for RPA results to present values closer to the photointerpretation reference data than to the fieldwork reference data because there is no cartographic uncertainty.

RPA classification results inside the field plot rectangles had their accuracy evaluated via Error Percentage [37], where zero Error Percentage means 100% accuracy, positive percentage values are omission errors, and negative percentage values are commission errors. For example, an Error Percentage of 5% means FR structural parameters lacked 5% of the reference data value (omission error), and an Error Percentage of −4% means FR structural parameters exceeded 4% of the reference data value (commission error). Equation (8) shows the calculation of Error Percentage, where "Reference" can be photointerpretation or fieldwork and "Results" are the RPA results automatically obtained.

The variation in Vegetation Cover and Grass Infestation in the experiment illustrated in Figure A2 was also calculated like Equation (8), but considering that "Reference" in Equation (8) is the "25 meters Measuring Tape" in Figure A2, and "Results" in Equation (8) is "Shift 2 meters East" or "Shift 2 meters West" in Figure A2. These variations in Vegetation Cover and Grass Infestation were measured for each field plot.

Appendix A.3. Results: RPA and Fieldwork Data Comparison Inside Field Plot Rectangles

Although Grass Infestation was the only FR structural parameter with medium accuracy as Section 3.1 shows, Table A1 shows some differences between RPA and fieldwork results. Such differences occurred because the RPA orthomosaic did not cover 33% of the whole field plots, as mentioned in Appendix A.1. Furthermore, stretches with non-vegetated and seedlings predominance (Nv and NvS in Figure 3) occupied 52.3% of the RPA study area, and these areas presented 21.4% of the field plots.

Table A1. RPA and fieldwork data comparison.

FR Structural Parameter	RPA	Fieldwork
Vegetation Cover (%)	27.80	55
Tree Density (trees/hectare)	814	1428
Tree Height (meters)	1.68	2
Grass Infestation (%)	27.57	25

When analyzing RPA results inside field plot rectangles, the Error Percentage was generally smaller with photointerpretation reference data than with fieldwork reference data, as Figure A3 shows.

Regarding Grass Infestation, a significant variation of its Error Percentage is presented in Figure A3. As Figure A4 shows, Grass Infestation may considerably vary if moving the measuring tape (or the 25-m line shapefile) two meters to the left or right, as described in Appendix A.1. Such variation reinforces remote sensing as a proper way for measuring Vegetation Cover and Grass Infestation.

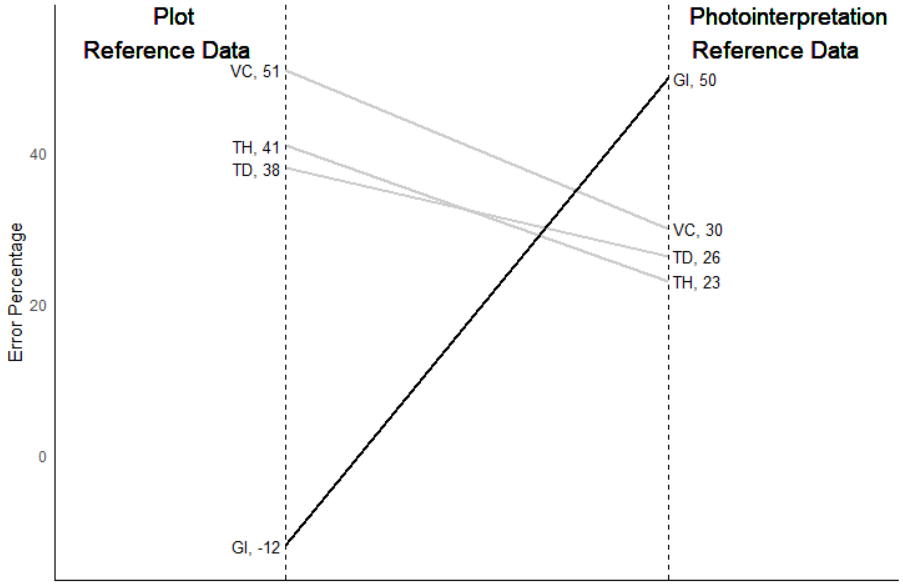

Figure A3. RPA results' Error Percentage inside field plots when considering two reference data: photointerpretation and fieldwork.

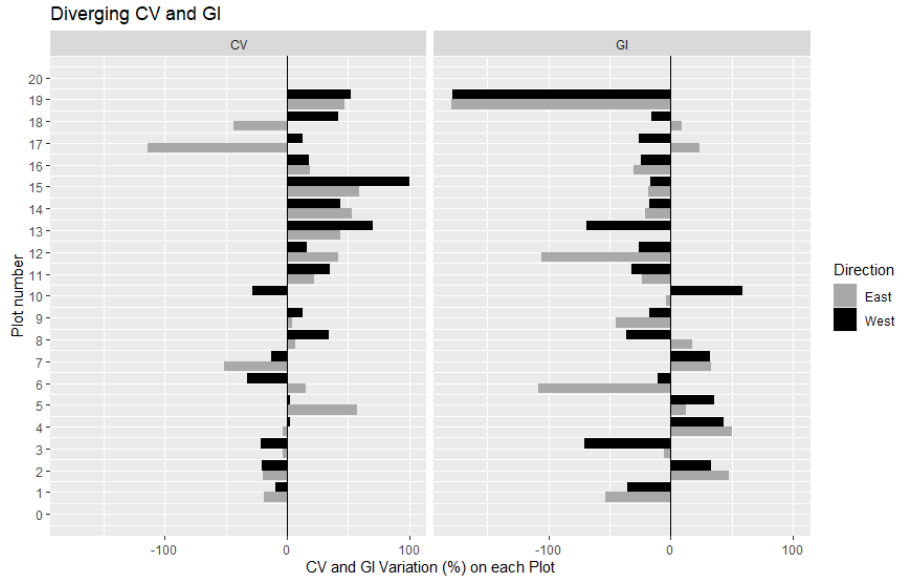

Figure A4. When measuring Vegetation Cover and Grass Infestation by a 25-m line shapefile, which is a simulation of the traditional fieldwork procedure, these FR structural parameters significantly varied when moving the measuring line 2 m in east and west directions. The registered Error Percentage presented mean and standard deviation equal to 11.48 ± 39.45 for Vegetation Cover and −20.3 ± 54.61 for Grass Infestation.

Appendix A.4. Discussion: Lessons Learned when Replicating Field Plots in RPA Imagery

RPA and fieldwork results differ when whole field plots are not overflown. RPA and fieldwork results presented quite some differences between them because 17.9% of the area analyzed by fieldwork was not included in the RPA study area. Despite such differences, RPA can contribute to the traditional fieldwork sampling process because it registers whole project areas, so it is possible to identify stretches with different FR success that lack or exceed field plot samples. For instance, stretches with grass predominance occupied 52.3% of the RPA study area, but presented 21.4% of the field plots.

Due to the cartographic uncertainty between fieldwork data and RPA imagery, the RPA results get closer to the photointerpretation than to the fieldwork data of each field plot. Error Percentage inside field plots was smaller with photointerpretation reference data than with fieldwork reference data, as Figure A3 shows. If both the RPA orthomosaic and the fieldwork data presented precise GNSS coordinates, the Error Percentage variation shown in Figure A3 would probably be smaller. However, one must consider that precise GNSS coordinates increase the fieldwork costs [50].

Measuring Vegetation Cover and Grass Infestation over RPA image by field plots procedure (25-m line) generates inconsistencies, reinforcing the RPA potential in measuring these variables by remote sensing techniques. Since Vegetation Cover and Grass Infestation are a two-dimension variable, measuring them by a line (one dimension) using RPA imagery is a source of many errors. The experiment of moving the line shapefile 2 m to the left and right showed significant variation in Vegetation Cover and Grass Infestation results, as illustrated in Figure A4. This fact confirmed that linear field measurements based on measuring tape should not be used in RPA images.

If the FR professionals wish to use precise GNSS coordinates to record the field plots location, they may consider turning the fieldwork rectangular plots into the Quadrat Method [61], which uses points. The Rio de Janeiro State official FR monitoring methodology has the option of using points instead of lines for field plots design. In these situations, each sampling point would be a precise GNSS coordinate (or also a ground control point of the RPA image), and the fieldwork analysts could collect the phytosociological data while the geodetic GNSS tracks its location. However, precise GNSS data usage increases the fieldwork costs [50].

Remote sensing and forest inventory are different sciences, but their final overall results must be similar. Although an obvious lesson, photointerpretation and traditional fieldwork presented some differences in this work because the whole FR area was not overflown. Furthermore, when trying to replicate field plots in the RPA image, the lack of precise GNSS coordinates also generated some differences between photointerpretation and fieldwork results. However, the two methodologies were able to state an ecological succession process in the study area.

References

1. Holton, A.E.; Lawson, S.; Love, C. Unmanned Aerial Vehicles: Opportunities, barriers, and the future of "drone journalism". *J. Pract.* **2015**, *9*, 634–650. [CrossRef]
2. Boursianis, A.D.; Papadopoulou, M.S.; Diamantoulakis, P.; Liopa-Tsakalidi, A.; Barouchas, P.; Salahas, G.; Karagiannidis, G.; Wan, S.; Goudos, S.K. Internet of things (IoT) and agricultural unmanned aerial vehicles (UAVs) in smart farming: A comprehensive review. *Internet Things* **2020**, 100187. [CrossRef]
3. Viani, R.; Rodrigues, R.; Padovezi, A.; Turini Farah, F.; Garcia, L.; Sanglade, L.; Brancalion, P.; Chaves, R.; Barreto, T.; Strassburg, B.; et al. Monitoring Protocol for Forest Restoration Programs & Projects. 2013; p. 61. Available online: https://www.researchgate.net/publication/304073085_Pacto_pela_restauracao_da_Mata_Atlantica_-_Protocolo_de_monitoramento_para_programas_e_projetos_de_restauracao_florestal (accessed on 17 June 2021).
4. Viani, R.A.; Holl, K.D.; Padovezi, A.; Strassburg, B.B.; Farah, F.T.; Garcia, L.C.; Chaves, R.B.; Rodrigues, R.R.; Brancalion, P.H. Protocol for monitoring tropical forest restoration: Perspectives from the Atlantic Forest Restoration Pact in Brazil. *Trop. Conserv. Sci.* **2017**, *10*, 1940082917697265. [CrossRef]
5. Aasen, H.; Burkart, A.; Bolten, A.; Bareth, G. Generating 3D hyperspectral information with lightweight UAV snapshot cameras for vegetation monitoring: From camera calibration to quality assurance. *ISPRS J. Photogramm. Remote Sens.* **2015**, *108*, 245–259. [CrossRef]
6. Zahawi, R.A.; Dandois, J.P.; Holl, K.D.; Nadwodny, D.; Reid, J.L.; Ellis, E.C. Using lightweight unmanned aerial vehicles to monitor tropical forest recovery. *Biol. Conserv.* **2015**, *186*, 287–295. [CrossRef]
7. McDonald, T.; Gann, G.; Jonson, J.; Dixon, K. *International Standards for The Practice of Ecological Restoration—Including Principles and Key Concepts*; Technical Report; Society for Ecological Restoration: Washington, DC, USA, 2016. Available online: http://www.seraustralasia.com/wheel/image/SER_International_Standards.pdf (accessed on 9 August 2019).
8. Myers, N.; Mittermeier, R.A.; Mittermeier, C.G.; Da Fonseca, G.A.; Kent, J. Biodiversity hotspots for conservation priorities. *Nature* **2000**, *403*, 853. [CrossRef] [PubMed]
9. Tarolli, P. High-resolution topography for understanding Earth surface processes: Opportunities and challenges. *Geomorphology* **2014**, *216*, 295–312. [CrossRef]

10. Mlambo, R.; Woodhouse, I.; Gerard, F.; Anderson, K. Structure from motion (SfM) photogrammetry with drone data: A low cost method for monitoring greenhouse gas emissions from forests in developing countries. *Forests* **2017**, *8*, 68. [CrossRef]
11. INEA. Manual de Procedimentos para o Monitoramento e Avaliação de áreas em Restauração Florestal no Estado do Rio de Janeiro. Technical Report, Instituto Estadual do Ambiente. 2019. Available online: http://www.inea.rj.gov.br/wp-content/uploads/2019/05/Manual-Monitoramento-%C3%81reas-Reflorestadas_WEB.pdf (accessed on 10 September 2019).
12. R Core Team. *R: A Language and Environment for Statistical Computing*; R Foundation for Statistical Computing: Vienna, Austria, 2013. Available online: http://www.R-project.org (accessed on 17 June 2021).
13. Agência Nacional de Aviação Civil (ANAC). Requisitos gerais para aeronaves não tripuladas de uso civil. Resolução número 419, de 2 de maio de 2017. Regulamento Brasileiro da Aviação Civil Especial, RBAC-E número 94, 2017. Available online: https://www.anac.gov.br/assuntos/legislacao/legislacao-1/rbha-e-rbac/rbac/rbac-e-94/@@display-file/arquivo_norma/RBACE94EMD00.pdf (accessed on 17 June 2021).
14. Albuquerque, R.W.; Costa, M.O.; Ferreira, M.E.; Carrero, G.C.; Grohmann, C.H. Remotely piloted aircraft imagery for automatic tree counting in forest restoration areas: A case study in the Amazon. *J. Unmanned Veh. Syst.* **2020**, *8*, 207–223. [CrossRef]
15. Júnior, L.R.A.; Ferreira, M.E.; Côrtes, J.B.R.; de Castro Jorge, L.A. High accuracy mapping with cartographic assessment for a fixed-wing remotely piloted aircraft system. *J. Appl. Remote Sens.* **2018**, *12*, 014003.
16. Hung, I.-K.; Unger, D.; Kulhavy, D.; Zhang, Y. Positional precision analysis of orthomosaics derived from drone captured aerial imagery. *Drones* **2019**, *3*, 46. [CrossRef]
17. Mohan, M.; Silva, C.; Klauberg, C.; Jat, P.; Catts, G.; Cardil, A.; Hudak, A.; Dia, M. Individual tree detection from unmanned aerial vehicle (UAV) derived canopy height model in an open canopy mixed conifer forest. *Forests* **2017**, *8*, 340. [CrossRef]
18. Liu, H.; Dong, P. A new method for generating canopy height models from discrete-return LiDAR point clouds. *Remote Sens. Lett.* **2014**, *5*, 575–582. [CrossRef]
19. Zhang, W.; Qi, J.; Wan, P.; Wang, H.; Xie, D.; Wang, X.; Yan, G. An easy-to-use airborne LiDAR data filtering method based on cloth simulation. *Remote Sens.* **2016**, *8*, 501. [CrossRef]
20. Silva, C.A.; Hudak, A.T.; Vierling, L.A.; Loudermilk, E.L.; O'Brien, J.J.; Hiers, J.K.; Jack, S.B.; Gonzalez-Benecke, C.; Lee, H.; Falkowski, M.J.; et al. Imputation of individual Longleaf Pine (*Pinus palustris* Mill.) Tree attributes from field and LiDAR data. *Can. J. Remote Sens.* **2016**, *42*, 554–573. [CrossRef]
21. Silva, C.A.; Crookston, N.L.; Hudak, A.T.; Vierling, L.A.; Klauberg, C.; Silva, M.C.A. Package 'rLiDAR'. 2017. Available online: https://cran.r-project.org/web/packages/rLiDAR/rLiDAR.pdf (accessed on 1 September 2019).
22. Oliveira, E.C.L.; Felfili, J.M. Estrutura e dinâmica da regeneração natural de uma mata de galeria no Distrito Federal, Brasil. *Acta Bot. Bras* **2005**, *19*, 801–811. [CrossRef]
23. Barbosa, B.; Ferraz, G.; Gonçalves, L.; Marin, D.; Maciel, D.; Ferraz, P.; Rossi, G. RGB vegetation indices applied to grass monitoring: A qualitative analysis. *Agron. Res.* **2019**, *17*, 349–357.
24. Reis, B.P.; Martins, S.V.; Fernandes Filho, E.I.; Sarcinelli, T.S.; Gleriani, J.M.; Leite, H.G.; Halassy, M. Forest restoration monitoring through digital processing of high resolution images. *Ecol. Eng.* **2019**, *127*, 178–186. [CrossRef]
25. Laliberte, A.S.; Browning, D.; Rango, A. A comparison of three feature selection methods for object-based classification of sub-decimeter resolution UltraCam-L imagery. *Int. J. Appl. Earth Obs. Geoinf.* **2012**, *15*, 70–78. [CrossRef]
26. Hunt, E.R.; Doraiswamy, P.C.; McMurtrey, J.E.; Daughtry, C.S.; Perry, E.M.; Akhmedov, B. A visible band index for remote sensing leaf chlorophyll content at the canopy scale. *Int. J. Appl. Earth Obs. Geoinf.* **2013**, *21*, 103–112. [CrossRef]
27. Grohmann, C.H.; Smith, M.J.; Riccomini, C. Multiscale analysis of topographic surface roughness in the Midland Valley, Scotland. *IEEE Trans. Geosci. Remote Sens.* **2010**, *49*, 1200–1213. [CrossRef]
28. Torres-Sánchez, J.; López-Granados, F.; Borra-Serrano, I.; Peña, J.M. Assessing UAV-collected image overlap influence on computation time and digital surface model accuracy in olive orchards. *Precis. Agric.* **2018**, *19*, 115–133. [CrossRef]
29. Colomina, I.; Molina, P. Unmanned aerial systems for photogrammetry and remote sensing: A review. *ISPRS J. Photogramm. Remote. Sens.* **2014**, *92*, 79–97. [CrossRef]
30. Schonberger, J.L.; Frahm, J.M. Structure-from-motion revisited. In Proceedings of the IEEE Conference on Computer Vision and Pattern Recognition, Las Vegas, NV, USA, 27–30 June 2016; pp. 4104–4113.
31. Crouzeilles, R.; Santiami, E.; Rosa, M.; Pugliese, L.; Brancalion, P.H.; Rodrigues, R.R.; Metzger, J.P.; Calmon, M.; Scaramuzza, C.A.D.M.; Matsumoto, M.H.; et al. There is hope for achieving ambitious Atlantic Forest restoration commitments. *Perspect. Ecol. Conserv.* **2019**, *17*, 80–83. [CrossRef]
32. Ferreira, M.P.; de Almeida, D.R.A.; de Almeida Papa, D.; Minervino, J.B.S.; Veras, H.F.P.; Formighieri, A.; Santos, C.A.N.; Ferreira, M.A.D.; Figueiredo, E.O.; Ferreira, E.J.L. Individual tree detection and species classification of Amazonian palms using UAV images and deep learning. *For. Ecol. Manag.* **2020**, *475*, 118397. [CrossRef]
33. Schiefer, F.; Kattenborn, T.; Frick, A.; Frey, J.; Schall, P.; Koch, B.; Schmidtlein, S. Mapping forest tree species in high resolution UAV-based RGB-imagery by means of convolutional neural networks. *ISPRS J. Photogramm. Remote Sens.* **2020**, *170*, 205–215. [CrossRef]
34. Florenzano, T.G. *Imagens de Satélite Para Estudos Ambientais*; Oficina de Textos: São Paulo, Brazil, 2002; p. 97.
35. Congalton, R.G. A review of assessing the accuracy of classifications of remotely sensed data. *Remote Sens. Environ.* **1991**, *37*, 35–46. [CrossRef]

36. Goutte, C.; Gaussier, E. A probabilistic interpretation of precision, recall and F-score, with implication for evaluation. In *European Conference on Information Retrieval*; Springer: Berlin/Heidelberg, Germany, 2005; pp. 345–359.
37. Keith, K.; Nicholson, D.; Rogers, D. Accuracy and precision of low-dose insulin administration using syringes, pen injectors, and a pump. *Clin. Pediatr.* **2004**, *43*, 69–74. [CrossRef]
38. Zhang, J.; Hu, J.; Lian, J.; Fan, Z.; Ouyang, X.; Ye, W. Seeing the forest from drones: Testing the potential of lightweight drones as a tool for long-term forest monitoring. *Biol. Conserv.* **2016**, *198*, 60–69. [CrossRef]
39. Nixon, M.; Aguado, A. *Feature Extraction and Image Processing for Computer Vision*; Academic Press: Cambridge, MA, USA, 2019; p. 626.
40. Braga, J.; Peripato, V.; Dalagnol, R.; Ferreira, M.; Tarabalka, Y.; Aragão, L.; de Campos Velho, H.; Shiguemori, E.; Wagner, F. Tree Crown Delineation Algorithm Based on a Convolutional Neural Network. *Remote Sens.* **2020**, *12*, 1288. [CrossRef]
41. Wagner, F.H.; Sanchez, A.; Tarabalka, Y.; Lotte, R.G.; Ferreira, M.P.; Aidar, M.P.; Gloor, E.; Phillips, O.L.; Aragao, L.E. Using the U-net convolutional network to map forest types and disturbance in the Atlantic rainforest with very high resolution images. *Remote Sens. Ecol. Conserv.* **2019**, *5*, 360–375. [CrossRef]
42. Wagner, F.H.; Sanchez, A.; Aidar, M.P.; Rochelle, A.L.; Tarabalka, Y.; Fonseca, M.G.; Phillips, O.L.; Gloor, E.; Aragão, L.E. Mapping Atlantic rainforest degradation and regeneration history with indicator species using convolutional network. *PLoS ONE* **2020**, *15*, e0229448. [CrossRef]
43. Ferreira, M.P.; Lotte, R.G.; D'Elia, F.V.; Stamatopoulos, C.; Kim, D.H.; Benjamin, A.R. Accurate mapping of Brazil nut trees (*Bertholletia excelsa*) in Amazonian forests using WorldView-3 satellite images and convolutional neural networks. *Ecol. Inform.* **2021**, *63*, 101302. [CrossRef]
44. Belmonte, A.; Sankey, T.; Biederman, J.A.; Bradford, J.; Goetz, S.J.; Kolb, T.; Woolley, T. UAV-derived estimates of forest structure to inform ponderosa pine forest restoration. *Remote Sens. Ecol. Conserv.* **2020**, *6*, 181–197. [CrossRef]
45. Chen, S.; McDermid, G.; Castilla, G.; Linke, J. Measuring vegetation height in linear disturbances in the boreal forest with UAV photogrammetry. *Remote Sens.* **2017**, *9*, 1257. [CrossRef]
46. Wu, X.; Shen, X.; Cao, L.; Wang, G.; Cao, F. Assessment of individual tree detection and canopy cover estimation using unmanned aerial vehicle based light detection and ranging (UAV-LiDAR) data in planted forests. *Remote Sens.* **2019**, *11*, 908. [CrossRef]
47. Camarretta, N.; Harrison, P.A.; Bailey, T.; Potts, B.; Lucieer, A.; Davidson, N.; Hunt, M. Monitoring forest structure to guide adaptive management of forest restoration: A review of remote sensing approaches. *New For.* **2020**, *51*, 573–596. [CrossRef]
48. Madasa, A.; Orimoloye, I.R.; Ololade, O.O. Application of geospatial indices for mapping land cover/use change detection in a mining area. *J. Afr. Earth Sci.* **2021**, *175*, 104108. [CrossRef]
49. Krause, S.; Sanders, T.G.; Mund, J.P.; Greve, K. UAV-based photogrammetric tree height measurement for intensive forest monitoring. *Remote Sens.* **2019**, *11*, 758. [CrossRef]
50. Ferrer-González, E.; Agüera-Vega, F.; Carvajal-Ramírez, F.; Martínez-Carricondo, P. UAV Photogrammetry Accuracy Assessment for Corridor Mapping Based on the Number and Distribution of Ground Control Points. *Remote Sens.* **2020**, *12*, 2447. [CrossRef]
51. Nie, Z.; Liu, F.; Gao, Y. Real-time precise point positioning with a low-cost dual-frequency GNSS device. *GPS Solut.* **2020**, *24*, 1–11. [CrossRef]
52. Martins, A.C.; Willig, M.R.; Presley, S.J.; Marinho-Filho, J. Effects of forest height and vertical complexity on abundance and biodiversity of bats in Amazonia. *For. Ecol. Manag.* **2017**, *391*, 427–435. [CrossRef]
53. Almeida, D.R.A.D.; Stark, S.C.; Chazdon, R.; Nelson, B.W.; César, R.G.; Meli, P.; Gorgens, E.; Duarte, M.M.; Valbuena, R.; Moreno, V.S.; et al. The effectiveness of lidar remote sensing for monitoring forest cover attributes and landscape restoration. *For. Ecol. Manag.* **2019**, *438*, 34–43. [CrossRef]
54. Ferreira, J.; Lennox, G.D.; Gardner, T.A.; Thomson, J.R.; Berenguer, E.; Lees, A.C.; Mac Nally, R.; Aragão, L.E.; Ferraz, S.F.; Louzada, J.; et al. Carbon-focused conservation may fail to protect the most biodiverse tropical forests. *Nat. Clim. Chang.* **2018**, *8*, 744–749. [CrossRef]
55. Wallace, L.; Lucieer, A.; Watson, C.S. Evaluating tree detection and segmentation routines on very high resolution UAV LiDAR data. *IEEE Trans. Geosci. Remote Sens.* **2014**, *52*, 7619–7628. [CrossRef]
56. Eugenio, F.C.; Schons, C.T.; Mallmann, C.L.; Schuh, M.S.; Fernandes, P.; Badin, T.L. Remotely piloted aircraft systems and forests: A global state of the art and future challenges. *Can. J. For. Res.* **2020**, *50*, 705–716. [CrossRef]
57. Schowengerdt, R.A. *Remote Sensing: Models and Methods for Image Processing*, 3rd ed.; Academic Press: Orlando, FL, USA, 2007; p. 515.
58. Alonzo, M.; Bookhagen, B.; Roberts, D.A. Urban tree species mapping using hyperspectral and lidar data fusion. *Remote Sens. Environ.* **2014**, *148*, 70–83. [CrossRef]
59. Araujo, L.; Vicente, L.E.; Manzatto, C.V.; Skorupa, L.A.; Victoria, D.D.C.; Soares, A.R. AgroTag: Um sistema de coleta, análise e compartilhamento de dados de campo para qualificação do uso e cobertura das terras no Brasil. In *Proceedings of Simpósio Brasileiro de Sensoriamento Remoto (SBSR), 19*; Gherardi, D.F.M., Sanches, I.D., e Cruz de Aragão, L.E.O., Eds.; INPE: São José dos Campos, Brazil, 2019; pp. 451–454.
60. Das, P.; Ortega, L.; Vilà-Valls, J.; Vincent, F.; Chaumette, E.; Davain, L. Performance Limits of GNSS Code-Based Precise Positioning: GPS, Galileo & Meta-Signals. *Sensors* **2020**, *20*, 2196.
61. Cottam, G.; Curtis, J.T. The use of distance measures in phytosociological sampling. *Ecology* **1956**, *37*, 451–460. [CrossRef]